

Spectroscopy of Superfluid Pairing in Atomic Fermi Gases

H.P. Büchler¹, P. Zoller¹, and W. Zwerger²

¹*Institute for Quantum Optics and Quantum Information of the Austrian Academy of Science, 6020 Innsbruck, Austria*

²*Institute for Theoretical Physics, Universität Innsbruck, 6020 Innsbruck, Austria*

(Dated: March 22, 2022)

We study the dynamic structure factor for density and spin within the crossover from BCS superfluidity of atomic fermions to the Bose-Einstein condensation of molecules. Both structure factors are experimentally accessible via Bragg spectroscopy, and allow for the identification of the pairing mechanism: the spin structure factor allows for the determination of the two particle gap, while the collective sound mode in the density structure reveals the superfluid state.

Atomic fermions have attracted a lot of interest as current cooling techniques allow for the creation of molecular condensates [1, 2, 3, 4]. These superfluids behave very much like standard Bose-Einstein condensates (BEC): the condensate may be inferred from the momentum distribution measured in a time of flight experiment. The tunability of the interaction through a Feshbach resonance then offers the possibility to explore the crossover from BEC of tightly bound molecules to the BCS superfluid state, where Cooper pairs only exist due to many body effects [5, 6, 7, 8, 9, 10]. Recent experiments have entered this regime [11, 12, 13], however, clear signatures for extended Cooper pairs in a BCS like ground state are missing so far. In this letter, we present a generalization of available spectroscopic tools to measure the dynamic structure factor for density and spin, which reveal important information on the pairing mechanism within the BEC-BCS crossover.

In conventional superconductors, the main characteristic properties are dissipation free transport and the Meissner-Ochsenfeld effect, which reveal themselves in the current response; density fluctuations are suppressed due to long-range Coulomb interactions [14] (see Ref. [8] for the current response in the BEC-BCS crossover). In contrast, for uncharged atomic gases transport measurements are not readily accessible due to the trapping potential. Then, the dynamic structure factors for density and spin are suitable quantities for the characterization of the superfluid ground state within the BEC-BCS crossover. Both quantities are accessible in traps: recent experiments measured the dynamic structure factor in interacting Bose gases via Bragg spectroscopy [15, 16, 17], while the dynamic spin susceptibility may be inferred by measuring the spin flip rate in stimulated Raman transitions [18, 19]. In this paper, we analyze the dynamic structure factor S_C and the dynamic spin structure factor S_s within the BEC-BCS crossover. We find, that the dynamic spin structure factor is dominated by processes which break paired fermions into two single particles and therefore reveals the many-body excitation gap. Furthermore, it provides the density of states, which signals the BCS pairing mechanism via the appearance of a van Hove singularity. The observation of this singularity was a fundamental indication for the validity of BCS theory

in conventional superconductors [14]. In turn, the superfluid transition is characterized by the appearance of a collective sound mode in the dynamic structure factor; this collective mode has recently been studied [10, 20, 21].

An interacting atomic gas of fermions with density $n_F = k_F^3/3\pi^2$ and two different spin states is characterized by the scattering length a_F allowing to tune the BEC-BCS crossover via the dimensionless parameter $1/(k_F a_F)$. As shown by Nozières and Schmitt-Rink [5], the BCS wave function becomes exact in the BCS limit ($1/(k_F a_F) \ll -1$) and the BEC limit ($1/(k_F a_F) \gg 1$). In the following, we use this BCS wave function to determine the dynamic structure factor S_C from the density response function χ_C , and the dynamic spin structure factor S_s from the spin susceptibility χ_s . This wave function accounts for the pairing between two fermions, while the residual interaction between unbound fermions providing particle-hole scattering is neglected. The interaction between molecules (Cooper pairs) is accounted for within Born approximation [6] (it is not necessary to introduce a molecular field as done in Ref. [10]). Within the BCS variational wave function, the fermionic normal Green's function \mathcal{G} and the anomalous Green's function $\mathcal{F}^+ = -\mathcal{F}$ take the standard form [14]

$$\mathcal{G}(\Omega_s, \mathbf{k}) = \frac{i\Omega_s + \epsilon_{\mathbf{k}}}{(i\Omega_s)^2 - E_{\mathbf{k}}^2}, \quad \mathcal{F}^+(\Omega_s, \mathbf{k}) = \frac{-i\Delta}{(i\Omega_s)^2 - E_{\mathbf{k}}^2}.$$

Here, $E_{\mathbf{k}} = \sqrt{\epsilon_{\mathbf{k}}^2 + \Delta^2}$ denotes the single-particle excitation energy with $\epsilon_{\mathbf{k}} = \hbar^2 \mathbf{k}^2 / 2m - \mu$ the free fermionic dispersion relation, while $\Omega_s = \pi T(2s+1)$ denotes fermionic Matsubara frequencies. The presence of a condensate and superfluid response in the ground state is encoded in a finite BCS gap Δ . The gap Δ is determined by the scattering length a_F via the gap equation, and the chemical potential is fixed by the particle density n_F [6],

$$-1 = \frac{4\pi\hbar^2 a_F}{m} \int \frac{d\mathbf{q}}{(2\pi)^3} \left[\frac{\tanh(\beta E_{\mathbf{q}}/2)}{2E_{\mathbf{q}}} - \frac{m}{\hbar^2 \mathbf{q}^2} \right], \quad (1)$$

$$n_F = 2 \int \frac{d\mathbf{q}}{(2\pi)^3} \left[\frac{1}{1 + e^{\beta E_{\mathbf{q}}}} \frac{\epsilon_{\mathbf{q}}}{E_{\mathbf{q}}} + \frac{E_{\mathbf{q}} - \epsilon_{\mathbf{q}}}{2E_{\mathbf{q}}} \right]. \quad (2)$$

In the BCS limit at low temperatures ($T = 0$), these relations give the chemical potential $\mu = \epsilon_F$ and the gap

$\Delta = \epsilon_F(8/e^2) \exp(\pi/2k_F a_F)$ with ϵ_F the Fermi energy. In turn, in the BEC limit the appearance of a two particle bound state with binding energy $\epsilon_0 = \hbar^2/(ma_F^2)$ and internal wave function $\phi_{\mathbf{k}} = (2n_F)^{-1/2}\Delta/E_{\mathbf{k}}$ modifies the chemical potential $\mu = -\epsilon_0/2$ and the gap $\Delta = \epsilon_0\sqrt{4\pi n_F a_F^3}$. Within the crossover regime, we solve Eq. (1) and (2) numerically to determine $\Delta(k_F a_F)$ and $\mu(k_F a_F)$. Note, that in general the BCS gap Δ differs from the two particle excitation gap $\Delta_s = \min_{\mathbf{k}} 2E_{\mathbf{k}}$.

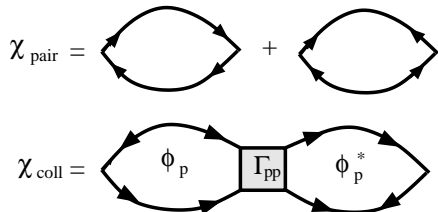


FIG. 1: Diagrams contributing to the density response function and the spin susceptibility; χ_{pair} accounts for particle-hole excitations, while the diagrams in χ_{coll} describe collective sound excitations.

In the following, we calculate the dynamic structure factor $S_C = -\text{Im}\chi_C/\pi$ and the dynamic spin structure factor $S_S = -\text{Im}\chi_S/\pi$ via their relations to the density response function and the spin susceptibility, respectively. The density response $\delta\rho_C(\omega, \mathbf{k})$ to a small external drive $\delta V_C(\omega, \mathbf{k})$ follows from $\delta\rho_C(\omega, \mathbf{k}) = \chi_C(\omega, \mathbf{q})\delta V_C(\omega, \mathbf{k})$ with the linear response function (in real space)

$$\chi_C(t, \mathbf{x}) = -i\Theta(t)\langle[\rho_C(t, \mathbf{x}), \rho_C(0, 0)]\rangle. \quad (3)$$

Here, $\langle\dots\rangle$ denotes the quantum statistical average at fixed temperature T and chemical potential μ , while the density operator is defined by $\rho_C = \psi_{\uparrow}^{\dagger}\psi_{\uparrow} + \psi_{\downarrow}^{\dagger}\psi_{\downarrow}$. The analogous definition applies for the spin susceptibility with the density ρ_C replaced by the spin density $\rho_S = \psi_{\uparrow}^{\dagger}\psi_{\uparrow} - \psi_{\downarrow}^{\dagger}\psi_{\downarrow}$. The diagrams contributing to the response functions χ_C and χ_S are shown in Fig. 1. Note, that each diagram has to be weighted by a nontrivial factor ± 1 . These factors differ for the response function χ_C and the spin susceptibility χ_S , and provide different cancellations between diagrams. We distinguish between two types of diagrams: The first type of diagrams χ_{pair} involve only normal and anomalous Green's function and describe two particle excitations, while the second type of diagrams χ_{coll} involve the vertex operator $\Gamma_{\alpha\beta}$ and account for collective excitations. The BCS wave function neglects particle-hole scattering and Γ accounts only for particle-particle (hole-hole) scattering. Then, $\alpha, \beta \in \{p, \bar{p}\}$ describe the incoming and outgoing type of particles; p accounts for particles and \bar{p} for holes. The vertex operator Γ has to be calculated with the help of the BCS wave function, see below. Note, that Fig. 1 shows only the diagram involving Γ_{pp} , while the other diagrams exhibit a similar structure. In the following, we are mainly interested in the zero temperature limit $T = 0$

and in the low momentum regime $k \ll 1/\xi = \Delta/\hbar c_s$ (the energy of the collective modes is below the two particle gap $\omega < \Delta_s$). Here, c_s denotes the macroscopic sound velocity and ξ the size of the pairs with $\xi \sim \hbar v_F/\Delta$ in the BCS limit and $\xi \sim a_F$ in the BEC limit. For typical experimental setups, the scale ξ is small compared to the trap size R , and we can safely assume the condition $1/R < k < 1/\xi$. Then, the trapping potential plays a minor role as has been shown in the measurement of the dynamic structure factor and the tunnelling probability, see Ref. [15, 16, 19]. Therefore, we ignore the influence of a trapping potential in the following analysis.

First, we focus on the spin susceptibility χ_S . At zero momentum, the spin susceptibility $\chi_S(\omega, 0)$ is equivalent to the response driven by the spin flip Hamiltonian $H = \lambda(t) \int d\mathbf{x} [\psi_{\uparrow}^{\dagger}\psi_{\downarrow} + \psi_{\downarrow}^{\dagger}\psi_{\uparrow}]$. A perturbation of this form is realized experimentally by driving a stimulated Raman transition between the two hyperfine states of the two component Fermi gas [19]. Within the diagrammatic expansion of χ_S , the diagrams in χ_{coll} cancel each other and only pair excitations χ_{pair} survive; their contribution takes the form

$$\chi_S(\Omega_s, \mathbf{k}) = -2T \sum_{t \in \mathbf{Z}} \int \frac{d\mathbf{q}}{(2\pi)^3} \left[\mathcal{G}(\Omega_t, \mathbf{q}) \mathcal{G}(\Omega_{s+t}, \mathbf{q} + \mathbf{k}) + \mathcal{F}^+(\Omega_t, \mathbf{q}) \mathcal{F}(\Omega_{s+t}, \mathbf{q} + \mathbf{k}) \right] \quad (4)$$

(Note, that for the density response function χ_C the + sign between the two terms is replaced by a - sign [14].) The integration in (4) involves standard methods, and we present here only the final result for the spin structure factor in the low momentum limit $k \ll 1/\xi$, see Fig. 2,

$$S_S(\omega) = \frac{3}{4} \frac{(n_F/\epsilon_F)\Delta^2}{\omega\sqrt{(\hbar\omega/2)^2 - \Delta^2}} \left[\frac{\sqrt{(\hbar\omega/2)^2 - \Delta^2 + \mu}}{\epsilon_F} \right]^{1/2}. \quad (5)$$

The spin structure factor exhibits a gap $\Delta_S = 2 \min_{\mathbf{k}} E_{\mathbf{k}}$, i.e., for positive μ the spin gap $\Delta_S = 2\Delta$ is determined by the BCS gap, while for $\mu < 0$, it is given by the binding energy $\Delta_S = 2\sqrt{\mu^2 + \Delta^2}$ approaching ϵ_0 in the BEC limit. The shape of the spin structure factor differs in the two limiting regimes: the shape exhibits the characteristic $1/\sqrt{\omega - 2\Delta}$ singularity of the density of states for the BCS pairing mechanism, while in the BEC regime S_S exhibits a maximum. In the crossover regime, Eq. (5) smoothly interpolates between these two limits. Next, we analyze the modifications of the spin structure factor for temperatures above the superfluid transition temperature T_c . Then, Eq. (1) implies $\Delta = 0$, and the spin structure factor in the BCS limit reduces to that of a Fermi gas. In turn, the presence of bound fermion pairs dominate the spin structure factor even above T_c ($T < T^*$) and S_S exhibits a pseudo gap $\sim \Delta_S \approx \epsilon_0$ with dissociated fermion pairs providing a small but finite weight within the gap. The pseudo gap finally disappears above

the pairing temperature $T > T^*$ via a smooth crossover. Therefore, the measurement of the spin structure factor provides a suitable tool for the characterization of the pairing temperature T^* and the spin gap Δ_s .

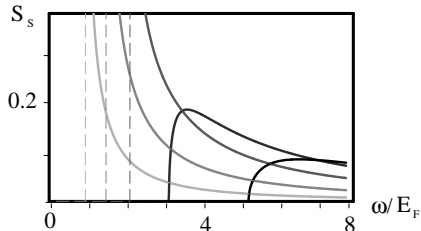


FIG. 2: Spin structure factor $S_s(\omega)$ in units $\hbar n_F/E_F$ for different scattering lengths $1/(a_F k_F) = -0.5, -0.25, 0, 0.25, 0.5$. The spin structure is quenched below the spin gap $\omega < \Delta_s$, and exhibits a characteristic singularity in the BCS limit.

In contrast, the dynamic density structure factor S_C in superfluids is dominated by a collective sound excitation representing the Goldstone mode of the broken symmetry (in conventional superconductors, Coulomb interactions lift this mode to the plasma frequency). The dynamic structure factor at low momenta $k \ll 1/\xi$ takes the form

$$S_C(\omega, \mathbf{k}) = n_F \frac{\hbar k}{2m c_s} \delta(\omega - c_s k) \quad (6)$$

exhausting the f -sum rule and compressibility sum rule,

$$\int_0^\infty d\omega \hbar \omega S_C(\omega, \mathbf{k}) = n_F \frac{\hbar^2 \mathbf{k}^2}{2m}, \quad (7)$$

$$\lim_{k \rightarrow 0} \int_0^\infty d\omega \frac{S_C(\omega, \mathbf{k})}{\hbar \omega} = \frac{n_F}{2m c_s^2}. \quad (8)$$

The determination of the sound velocity within the BEC-BCS crossover requires the calculation of the diagrams χ_{coll} in Fig. 1; its contribution exhausts the sum rules (7) and (8) at small momenta $k \ll 1/\xi$ and frequencies $\hbar\omega < \Delta_s$ i.e., a cancellation appears between χ_{pair} and χ_{coll} at frequencies $\omega > \Delta_s$. The diagrams in χ_{coll} provide the response function

$$\chi_C(\omega, \mathbf{k}) = 4 \sum_{\alpha, \beta} \phi_\alpha^*(\omega, \mathbf{k}) \Gamma_{\alpha, \beta}(\omega, \mathbf{k}) \phi_\beta(\omega, \mathbf{k}), \quad (9)$$

where one factor 2 accounts for summation of spin indices, while the second factor 2 appears as each vertex operator $\Gamma_{\alpha\beta}$ contributes to two diagrams. Using the microscopic approach by Haussmann [7], the vertex operator $\Gamma_{\alpha\beta}$ takes the form

$$(\Gamma_{\alpha\beta})^{-1} = \left[\frac{m}{4\pi \hbar^2 a_F} - \int \frac{d\mathbf{k}}{(2\pi)^3} \frac{m}{\hbar^2 \mathbf{k}^2} \right] \delta_{\alpha\beta} + M_{\alpha\beta} \quad (10)$$

with

$$M_{pp}(\Omega_s, \mathbf{k}) = T \sum_{t \in \mathbb{Z}} \int \frac{d\mathbf{q}}{(2\pi)^3} [\mathcal{G}(\Omega_{s-t}, \mathbf{q} + \mathbf{k}) \mathcal{G}(\Omega_t, -\mathbf{q})],$$

$$M_{p\bar{p}}(\Omega_s, \mathbf{k}) = T \sum_{t \in \mathbb{Z}} \int \frac{d\mathbf{q}}{(2\pi)^3} [\mathcal{F}(\Omega_{s-t}, \mathbf{q} + \mathbf{k}) \mathcal{F}(\Omega_t, -\mathbf{q})],$$

with $M_{pp} = M_{\bar{p}\bar{p}}^*$ and $M_{p\bar{p}} = M_{\bar{p}p}^*$. The propagators ϕ_p^* (ϕ_p) account for the creation (destruction) of a fermion pair from the condensate, and take the form

$$\phi_p = T \sum_t \int \frac{d\mathbf{q}}{(2\pi)^3} \mathcal{G}(\Omega_t, \mathbf{q}) \mathcal{F}(\Omega_{t+s}, \mathbf{q} + \mathbf{k}). \quad (11)$$

Solving the above equations in the limit of small frequency $\omega \ll \Delta_s$ and momenta $k \ll 1/\xi$ provides the collective sound mode with sound velocity c_s ; the result is shown in Fig. 3.

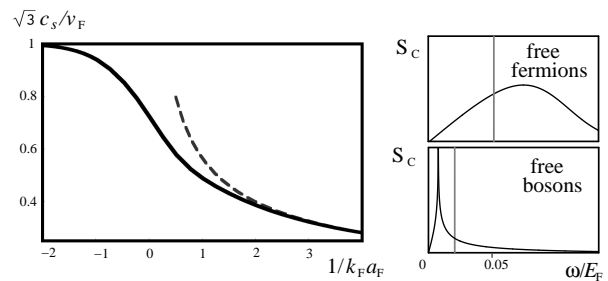


FIG. 3: Left: Sound velocity c_s in the BEC-BCS crossover in units $v_F/\sqrt{3}$. The dashed line is the Bogoliubov sound velocity. Right: Structure factor $S_C(\omega)$ of weakly interacting fermions and bosons above the superfluid transition temperature $T = \epsilon_F/2 > T_c$ and $k = \sqrt{3}k_F/40$. The gray line denotes the peak of the sound mode below the superfluid transition.

Within the BCS limit, the collective excitations (9) provide the Bogoliubov-Anderson sound mode for a neutral superconductor with $c_s = v_F/\sqrt{3}$ [22]. The particle-hole contributions, dominating the structure factor for a weakly interacting Fermi gas, are quenched due to the opening of the excitation gap. Note, that the leading correction to the sound velocity $c_s = v_F/\sqrt{3}[1 - 8k_F a_F/\pi]$ derives from particle-hole scattering [22]; such scattering processes are not contained in our approach. In turn, within the BEC limit Eq. (9) gives the structure factor $S_C^{\text{BEC}}(\omega, \mathbf{k}) = 2n_F \delta(\omega - \hbar \mathbf{k}^2/4m)$. The variational BCS wave function approach provides the zeroth order result describing a noninteracting Bose gas of molecules with density $n_B = n_F/2$ and mass $m_B = m/2$. The structure factor becomes 4 times the structure factor of an ideal Bose gas. This factor 4 appears as the external potential drives the fermionic density operator instead of the bosonic density operator; the structure factor satisfies the f -sum rule for fermions with $n_F/m = 4n_B/m_B$. Going beyond leading order, the above equations also incorporate the repulsion between the bound pairs, and provide the structure factor $S_C^{\text{BEC}}(\omega, \mathbf{k}) = 2n_F \tilde{\epsilon}_{\mathbf{k}} / \tilde{E}_{\mathbf{k}} \delta(\omega - \tilde{E}_{\mathbf{k}}/\hbar)$ with $\tilde{\epsilon} = \hbar^2 \mathbf{k}^2 / 2m_B$ and the Bogoliubov excitation spectrum $\tilde{E}_{\mathbf{k}}^2 = \tilde{\epsilon}_{\mathbf{k}}^2 + 2\mu_B \tilde{\epsilon}_{\mathbf{k}}$. The structure factor describes a weakly interacting Bose gas with sound velocity $c_s = \sqrt{\mu_B/m_B}$. Here, $\mu_B = 4\pi \hbar^2 a_B n_B / m_B$ denotes the bosonic chemical potential accounting for the scattering length $a_B = 2a_F$ within Born approximation; its exact value $a_B \approx 0.6$ has recently been derived [23].

Next, we focus on the dynamic structure factor above the superfluid transition temperature $T > T_c$ and compare it with the structure factor Eq. (6). We first focus on the collisionless regime $\omega\tau > 1$ with τ the collision time; this limit is naturally achieved for weakly interacting atomic gases ($|k_F a_F| < 1$) and frequencies ω above the trapping frequency [24]. Within the BCS limit, the system reduces to a Fermi liquid with a weak attractive interaction. The structure factor exhibits the particle-hole excitation spectrum of a weakly interacting Fermi gas at finite temperature (interactions only renormalize the Fermi velocity v_F), while the zero sound mode is overdamped for attractive fermions; the structure factor is shown in Fig. 3. In turn, in the BEC limit the system above the critical temperature T_c reduces to a gas of bosonic molecules. The structure factor of a degenerate Bose gas with temperatures above the superfluid transition temperature derives from the bosonic Lindhard function; the structure at low momenta is shown in Fig. 3. Comparing these structure factors with Eq. (6), we find that the superfluid state is characterized by the appearance of a collective sound mode. However, for the system in the hydrodynamic regime $\omega\tau < 1$, the structure factor is exhausted by the hydrodynamic sound mode (first sound) even above the superfluid transition. Therefore, the identification of the superfluid transition from the density response requires to be in the collisionless regime, which is reached for sufficiently weak interactions.

Within recent experiments [2, 13], the molecular binding energy in the BEC limit was determined by a r.f. pulse breaking the molecules and exciting a fermion into a different hyperfine state. This method has the disadvantage that the interactions between the fermions in different hyperfine states produces non-trivial energy shifts. In turn, the structure factors presented here, produce excitations within the same hyperfine states. However, the two hyperfine states are separated by an energy $\hbar\omega_{\uparrow\downarrow}$ due to Zeeman splitting. Using a driving field at frequency $\omega_{\uparrow\downarrow}$ with an additional superimposed modulation frequency ω , i.e., $\lambda(t) \sim \cos(\omega_{\uparrow\downarrow}t)\cos(\omega t)$, then probes the structure factors $S_s(\omega)$ with the number of particles in each hyperfine state conserved. Such a procedure avoids non-trivial energy shifts induced by a change in particle number or excitation of particles into different hyperfine state, and therefore represents a suitable setup for a determination of the two particle excitation gap Δ_s . The measurement of the structure factors can be achieved in two different ways: First, the energy transfer W to the system satisfies $W = \gamma\omega S(\omega, \mathbf{k})$ with γ determined by the driving field alone and allows for the determination of S from the heating of the system [15, 16]. For ${}^6\text{Li}$, the characteristic parameters at the Feshbach resonance are given by $\Delta_s \sim E_F \sim 1\mu\text{K}$ and $\omega_{\uparrow,\downarrow} \sim 80\text{MHz}$, i.e., the structure factor is accessible via Raman transitions or r.f. pulses as and shown in recent experiments [2, 13, 19]. Second, the interaction between the driving

field and the fermions leads to the absorption and emission of photons with a rate determined by the structure factor $S(\omega, \mathbf{k})$. Therefore, an analysis of the counting statistic of the probing laser field allows for an *in-situ* measurement of the structure factors.

We thank G. Blatter, A. Recati, R. Grimm and C. Chin for stimulating discussions. Work at the University of Innsbruck is supported by the Austrian Science Foundation, European Networks, and the Institute of Quantum Information.

-
- [1] S. Jochim, M. Bartenstein, A. Altmeyer, G. Hendl, S. Riedl, C. Chin, J. H. Denschlag, and R. Grimm, *Science* **302**, 2101 (2003).
 - [2] M. Greiner, C. A. Regal, and D. S. Jin, *Nature* **426**, 537 (2003).
 - [3] M. W. Zwierlein, C. A. Stan, C. H. Schunck, S. M. F. Raupach, S. Gupta, Z. Hadzibabic, and W. Ketterle, *Phys. Rev. Lett.* **91**, 250401 (2003).
 - [4] T. Bourdel, L. Khaykovich, J. Cubizolles, J. Zhang, F. Chevy, M. Teichmann, L. Tarruell, S. J. J. M. F. Kokkelmans, and C. Salomon, *cond-mat/0403091* (2004).
 - [5] P. Nozières and S. Schmitt-Rink, *J. Low Temp. Phys.* **59**, 195 (1985).
 - [6] M. Randeria, J.-M. Duan, and L.-Y. Shieh, *Phys. Rev. B* **41**, 327 (1990); J. R. Engelbrecht, M. Randeria, and C. A. R. Sá de Melo, *Phys. Rev. B* **55**, 15153 (1997).
 - [7] R. Haussmann, *Z. Phys. B* **91**, 291 (1993).
 - [8] F. Pistolesi and G. C. Strinati, *Phys. Rev. B* **49**, 6356 (1994); N. Andrenacci, P. Pieri, and G. C. Strinati, *Phys. Rev. B* **68**, 144507 (2003).
 - [9] M. Holland, S. J. J. M. F. Kokkelmans, M. L. Chiofalo, and R. Walser, *Phys. Rev. Lett.* **87**, 120406 (2001).
 - [10] Y. Ohashi and A. Griffin, *Phys. Rev. Lett.* **89**, 130402 (2002); Y. Ohashi and A. Griffin, *Phys. Rev. A* **67**, 063612 (2003).
 - [11] C. A. Regal, M. Greiner, and D. S. Jin, *Phys. Rev. Lett.* **92**, 040403 (2004).
 - [12] M. W. Zwierlein *et al.*, *Phys. Rev. Lett.* **92**, 120403 (2004).
 - [13] R. Grimm *et al.*, to be published.
 - [14] J. R. Schrieffer, *Theory of superconductivity* (Frontiers in Physics, 1964).
 - [15] D. M. Stamper-Kurn *et al.*, *Phys. Rev. Lett.* **83**, 2876 (1999).
 - [16] J. Steinhauer, R. Ozeri, N. Katz, and N. Davidson, *Phys. Rev. Lett.* **88**, 120407 (2002).
 - [17] T. Stöferle *et al.*, *cond-mat/03312440* (2003).
 - [18] P. Törmä and P. Zoller, *Phys. Rev. Lett.* **85**, 487 (2000).
 - [19] R. Grimm and C. Chin (private discussion).
 - [20] A. Minguzzi, G. Ferrari, and Y. Castin, *Eur. Phys. J. D* **17**, 49 (2001).
 - [21] W. Hofstetter *et al.*, *Phys. Rev. Lett.* **89**, 220407 (2002).
 - [22] P. W. Anderson, *Phys. Rev.* **112**, 1900 (1958).
 - [23] D. S. Petrov, C. Salomon, and G. V. Shlyapnikov, *cond-mat/0309010* (2003).
 - [24] L. Pitaevskii and S. Stringari, *Bose-Einstein condensation* (Oxford Scientific Publications, 2002).